1, 2.5 and/or 3D Inversion of Airborne EM data - options in the search for sediment-hosted base metal mineralisation in the McArthur Basin, Northern Territory.

Tim Munday*
CSIRO Mineral Res
Perth, WA, Australia
tim.munday@csiro.au

Camilla Soerensen
CSIRO Mineral Res
Perth, WA, Australia
camilla.soerensen@csiro.au

Dave Marchant
Computational Geosc. Inc.
Vancouver, Canada
dave@compgeoinc.com

Jovan Silic
Jovan Silic & Assoc.
Melbourne, VIC
jsilic@bigpond.com

Rod Paterson
Intrepid Geophysics
Melbourne, Vic
rod@intrepid-geophysics.com

Andrea Viezzoli
Aarhus Geophysics Aps
Pisa, Italy
andrea.viezzoli@aarhusgeo.com

Marcus Kunzmann
CSIRO Mineral Res
Darwin, NT, Australia
marcus.kunzmann@csiro.au

Sam Spinks
CSIRO Mineral Res
Perth, WA, Australia
sam.spinks@csiro.au

SUMMARY

The southern McArthur Basin in Australia's Northern Territory is host to some Tier-1 sediment-hosted base metal mineral deposits including the McArthur River Zn-Pb-Ag mine. Airborne electromagnetic (AEM) data sets have been employed as a key exploration technology in the search for these mineral systems. A geological interpretation of results arising from the use of different inversion techniques, including a 1, 2.5 and 3D methods, was undertaken on a helicopter EM data set acquired over a structurally complex sediment package in the Batten Fault Zone north of the McArthur River Mine. The exploration targets were conductive, mineralised units (HYC pyritic shale member) associated with the Barney Creek Formation. Results from this study suggested that although the model fits were good, the derived conductivity models for the 2.5D and 3D inversions appeared to be smooth representations of geological reality, particularly when compared with data from drilling and surface geological mapping. Superficially, the 1D smooth model layered Earth inversions appear to map geological variability and structural complexity in greater detail even though the structures are more 3D in nature. IP effects are observed in the data and influence the modelled structure, but can be accounted for and complement the non IP 1D inversion results. The outcome of this study also indicates that when employing higher order inversion methods in the interpretation of AEM data sets, there may be significant benefit in asking a contractor/consultant for 1D inversion results as well. In the resulting interpretations if conductors appear in one but not the other, it is worth asking the question why?

Key words: AEM inversion, 1D, 2.5D, 3D, Airborne IP, McArthur Basin, Base metal mineral systems

INTRODUCTION

The southern McArthur Basin in Australia's Northern Territory (Figure 1), has been the focus for exploration for base-metal bearing pyritic shale units. The potential for time domain electromagnetic (TDEM) systems to assist the exploration for units was recognised in the early 1990s with results emerging from QUESTEM and GeoTEM fixed wing, time domain EM data acquired over the McArthur River (HYC) Zn-Pb-Ag deposit. Both systems produced clear anomalies over the deposit (Shalley and Harvey 1992). This success was a spur to more extensive AEM data acquisition programs across the McArthur Basin with particular focus on the Batten Fault Zone (Figure 1). AEM systems continue to be employed for exploration throughout the basin, although the challenges of exploration at depth (>500m) remain a perceived challenge by the exploration community, even though more powerful (higher moment, lower noise) AEM systems are now routinely available.

From a base metal exploration perspective, targets for AEM systems in the McArthur Group are primarily the conductive, very fine-grained, thinly bedded sulphide ore-bearing shale and dolomitic siltstone intervals, commonly referred to as the HYC Pyritic Shale Member of the Barney Creek Formation. Their identification was the principal objective for the AEM survey undertaken over the Caranbirini project area in the Batten Fault Zone; the focus for this study (Figure 1). Prior geological and structural investigations over the study area (e.g. Ahmad *et al.*, 2013; Betts *et al*., 2015) indicated the presence of a complex basin architecture with NNW-SSE orientated folds and faults in shale-bearing units of the McArthur Group, west of the Emu Fault (Figure 2). In this paper we examine the relative merits of different EM inversion approaches for resolving the HYC Pyritic Shale Member using heli-borne TDEM data, and specifically consider results from application of 1D, 2.5D and 3D EM inversion methods using algorithms in common use by the exploration community. The intent was to assess their value in mapping the location, geometry and extent of conductive parts of the Barney Creek Formation at depth, particularly where the sediment package is known to be faulted and folded.

1D Layered Earth Inversion (LEI) algorithms assume that the earth is represented by a set of one dimensional layers, extending to an infinite distance in the horizontal plane. However, this assumption has its limits, demonstrated to create artefacts when applied to a heterogeneous three dimensional geology (e.g. Ellis, 1998 and Yang and Oldenburg, 2012). Arguably in the geological complex environment encountered in the study area, AEM survey data might be best interpreted using 2.5D or 3D methods as they better model the physics involved in a decaying EM signal as it diffuses through the earth. However, until more recently the prospect of inverting the large volumes characterized by airborne EM datasets was often considered too time consuming given the processing complexities

and computational overheads involved in 2.5 and 3D approaches. These challenges have been addressed through, for example, a new forward model algorithms and a new 2.5D inversion solver with adaptive regularisation (see Silic *et al.*, 2015); the use of a moving footprint to limit the number of data points required in calculating the large sensitivity matrix needed as input to a 3D inversion at any one location (see Cox *et al.*, 2010); and by partitioning the forward problem into multiple meshes, resulting in a forward modelling mesh that has far fewer cells than the full inversion mesh thereby reducing the bottleneck for 3D AEM inversions (see Yang *et al*., 2014).

METHOD

AEM system and survey

A total of ~900 line kms of data were considered, having been acquired with the VTEM helicopter TDEM system along E-W oriented lines across the study area with a line spacing of 200m (Figure 2). System characteristics for the VTEM system are summarised in Figure 3.

Inversion approaches

Three inversion approaches were examined, and consideration was also given to inverting for airborne induced polarisation (AIP) and resistivity, as the Caranbirini VTEM data set contained AIP effects. AIP effects have been reported in other time-domain helicopter airborne electromagnetic (AEM) data primarily as a consequence of advances in instrumentation, resulting in improvements in the signal-to-noise ratio and hence better data quality (see, for example, Kaminski and Viezzoli, 2017).

1D Inversion

The 1D inversion scheme AarhusInv (Auken *et al*., 2015) was used in the Aarhus Workbench to process and invert the VTEM data. The data were processed manually to remove noise and IP effects. The AarhusInv algorithm inverts soundings for a set of 1D models connected through constraints. The inversion requires a data file as well as a model input definition file containing information on starting model, regularization constraints as well as any prior information. For the purposes of this study, a 30 layer model was used for the inversion employing Z component data. The first layer thickness was chosen to be 10m with logarithmically increasing thicknesses to a depth of 1500m, which is the depth of the last layer boundary. The starting model for the inversion was a homogenous halfspace with a resistivity of 40 ohm. A depth of investigation (DOI) was also defined using the method of Christiansen and Auken (2012).

1D Inversion for Airborne IP Effects and Resistivity

Induced polarization (IP) effects are evident in the VTEM data acquired over Caranbirini and are manifest as negative receiver voltage values, which in some cases are easy to detect. However, they can also be present in these data as exceedingly fast decays, or erratic slopes/curvatures, without ever changing sign. Smith (2016) refers to such behaviour as 'shape reversals', where a high spatial frequency feature changes from a relative positive at early times to a relative negative at late times. In some cases, the most subtle IP effects will not become evident until modelling is attempted. Some shape reversals could be misinterpreted as 3D effects, so care must be given to their study in data space, accompanied by an assessment of inversion outputs in the model space. AIP modelling starts from thorough visual analysis of the data, and different metrics are used to assist in the assessment of the AIP effects spatially and against known geology (see Manca and Viezzoli, 2018). The data are then processed, deleting noisy gates, while retaining undistorted IP effects. The 1D inversion with IP modelling was carried out with AarhusInv, with Laterally Constrained Inversion (LCI). All four Cole Cole parameters ("IP corrected" ρ_{dc}, chargeability *m*, frequency parameter *c*, time constant τ) are solved for, at once, with spatial constraints of varying strengths. Care must be exerted in proper sampling of the regularization/starting model space. If needed, further post-processing is carried out. Notice that, even if one was not interested in chargeability, the "IP corrected" ρ_{dc}, resulting from this AIP modelling process can provide additional insights into geological modelling and exploration.

At the time of writing, the 2.5D and 3D inversion codes employed here were unable to model AIP. Its presence can lead to significant artefacts in the resulting model if they are not first identified and removed. Therefore, for these two methods, soundings affected by IP were manually identified and removed from the data set prior to inversion. Where possible, only late time channels were removed from the inversion. It needs to be stressed however, that AIP effects do not affect "late times" only (e.g., Smith 1989, Flis *et al.*, 1989 and Viezzoli *et al*., 2016), but rather distort large portions of the entire transient. It is therefore virtually impossible to eliminate them totally from the measured data prior to inversion.

2.5D Inversion

A 2.5D inversion of the VTEM data using the Moksha code was undertaken by Intrepid Geophysics. The inversion code used in this work has been described by Paterson *et al.*, (2016), and Silic *et al*., (2015), and comprises a significantly re-engineered version of ArjunAir (Wilson *et al*., 2006). Among the changes is a new forward model algorithm (ArjunAir only produced accurate results for layer models), and a new 2.5D inversion solver with adaptive regularisation which allows the incorporation of a misfit to the reference model and the model smoothness function. The regularisation parameter is chosen automatically and changed adaptively at each iteration, as the model, the sensitivity and the roughness matrices change (Silic *et al*., 2015). The estimation of regularisation parameter requires calculation of only one forward model and sensitivity matrix at each iteration and is controlled by an easily understood parameter - the Relative Singular Value Truncation (RSVT) parameter. In contrast to ArjunAir the 2.5D inversion can be executed on multi CPU parallel processing platforms. In this study, Z component data were inverted with the inversion using 10m stations, with a 30-40m (lateral dimension) mesh, and a 5m mesh at surface increasing with depth down to 750 m.

3D Inversion

The 3D inversion of the Caranbarini VTEM dataset was undertaken by Computational Geosciences Inc., using an adaptive OcTree mesh refinement, where the mesh spans the full computational domain but uses smaller mesh cells around the selected transmitters and receivers. This mesh refinement methodology results in a forward modelling mesh that has far fewer cells than the full inversion mesh. This procedure results in a highly parallel 3D inversion algorithm that can handle large datasets. It builds on the approach described by Haber *et al*., (2012), Schwarzbach *et al*., 2013, and Yang *et al.,* (2014). For this project, the OcTree mesh's smallest cells were 25m x 25m x 25m. These fine cells were used to mesh the topography, the air surrounding the transmitter and receiver locations and the top 300m of the subsurface. Below 300m the cells expand by a factor of two with each 300m of depth. This discretization scheme resulted in an inversion mesh consisting of approximately 9.25 million cells (5,406,552 cells discretising the earth, 3,846,372 cells discretising the air).

RESULTS

Limited, deep (~1000m) drilling is available in the study area, permitting the geological interpretation of the results generated from the inversions. An example is shown in Figure 4 for DD83CA3 - a diamond hole located just to the west of the Emu Fault on VTEM flight line 10460 (Figure 2). A 1D model for the fiducial closest to the hole suggests that the Barney Creek Formation is conductive, and a resistivity log for the same hole indicates that the interpreted HYC Pyritic Shale Member of that formation exhibits high conductivities. The location of the drill hole and related stratigraphy are shown overlain on a 1D smooth model LEI of Line 10460 in Figure 5. This conductivity-depth section identifies a very conductive near-surface package east of the Emu Fault which is associated with Cambrian sediments. The cause for the observed high conductivities remains undetermined but may be groundwater related (i.e. saline groundwater). West of the Emu Fault, more moderate, folded and sub-horizontal, conductors are identified between 2000 and 6000m along the line at elevations between -200 and -500mAHD. We attribute these features to folded and faulted section of the McArthur Group of sediments, including the Barney Creek Formation. This attribution results from an analysis of lithological data from other drill holes in the area. For example, core from a diamond drill hole (MANT-79-2) on line 10470 (not shown) intersects what is interpreted as the HYC pyritic shale unit (based on carbon isotope chemostratigraphy) coincident with the presence of these folded conductors defined in the 1D inversion results. They also coincide with folds identified in surface mapping (see Figure 2).

The 1D results could be interpreted to resolve a structurally contorted sediment package that might relate to transpression, faulting and uplift of part of the McArthur Group in this location. The disruption of the lateral extension of the conductive unit associated with the interpreted HYC shale unit may also indicate the presence of growth (?) faults (potentially important conduits for mineralised fluids). Similar structures are observed in the flight line further south (Line 10440) (Figure 6), and on additional lines to the north and south. The synclinal conductor centred at ~2500m in Figure 5, might be interpreted as the westward extension of the HYC pyritic shale member. Overall, observations from several drill holes across the survey area support the interpretation that the HYC shale unit is laterally extensive and variably conductive. Examination of sections from the 2.5D and 3D inversions (Figure 6) indicates that the conductive units west of the Emu Fault are either poorly resolved or non-existent. Both higher order inversions appear to generate a smoothed view of the subsurface. Both the 2.5D and 3D results identify the presence of a broad, eastwards-dipping conductor (between 2500 and 4500m), a conductor which is also present in the 1D results whether inverted for IP or not (Figure 5 & 7).

Previously, it has been argued that undulating conductors observed in the 1D sections (Figure 5 & 7) are artefacts in the 1D inversion, a consequence of "variable near-surface overburden features" (*cf.* Silic *et al.*, 2017), but given their close correspondence with the geology (including the Barney Creek Formation) mapped at surface, and from drilling, it suggests they most likely reflect the geological structure. All the inversions identify a conductive, but variable, near surface unit which we interpret as a conductive regolith. When the VTEM data are inverted for resistivity (1D) and IP ((there some clear negatives in the transients), the results indicate that some of the near surface regolith materials exhibit a chargeable response (Figure 7). The conductivity structure obtained whilst modelling IP largely confirms the standard, non-IP 1D inversions results, with the main difference being the absence of a deep conductive layer toward the middle of the section, which was present just above DOI in the standard 1D inversion. The presence of a dipping conductive unit at the western end of the line (at around -400mAHD, between 3000 and 4500m in Figure 6 and 7) in the 1D results, is also reflected in the 2.5 and 3D inversion results, confirms its likely presence.

Drilling undertaken by CRA in the early 1980's intersected the mineralised HYC pyritic shale member of the Barney Creek Formation on lines 10440 and 10460 (Figures 2, 5 – drillhole DD83CA3 and Figure 6), adjacent to the Emu Fault. The presence of this unit coincides with a moderate, westerly dipping, deep conductor defined in the 1D inversion results between 7500 and 8500m along these lines (Figure 5). The presence of the same, but smoother, and broader conductor in the 3D results (between 7500 and 8500m), arguably supports the observation that the 1D code is resolving a conductive unit at this location (Figure 8). While the 2.5D results hint at the presence of this small conductor (Figure 6 and 8), it is not defined. Silic *et al.* (2017) suggested that the 1D results were simply identifying "… an off-end effect from large fault conductor". Discussion continues as to whether the mineralised HYC unit is resolvable with 1D inversion methods at this depth, or even whether the VTEM system would be able to detect a moderate conductor of this type at this depth. Further work is required to resolve these issues more conclusively.

CONCLUSIONS

In the study area, results from the 1D smooth model LEI's (whether IP effects are accounted for or not) appear to map geological variability and structural complexity in greater detail compared to those from the 2.5D and 3D inversions, even though the geology is more 3D in nature. This supports observations made in comparable studies (e.g. Costelloe *et al*., 2013), although recent work reported by Paterson *et al.* (2017) suggested that the 2.5D code shows "superior outcomes with regard to dip, thickness, conductive and resistive property extremes and a depth sensitivity at least 25 per cent greater than the traditional 1D methods". Results presented here are less

conclusive for the targets of relevance to base metal exploration in the McArthur Basin. Here we suggest that while the overall model fits were good, the derived geological models for the 2.5D and 3D inversions appeared to be either smooth, or more simplified versions of geological reality. To-date, neither the 2.5 nor the 3D inversion methods have always been able to resolve the presence of, or detail associated with conductive sedimentary units (the HYC pyritic shale unit) where it has been mapped in drilling across the study area. In the case of the 2.5D model results, the presence of the HYC pyritic shale unit identified from drilling on the western side of the Emu Fault was not determined, whereas the 1D (with and without IP accounted for) and 3D inversion appear to map a conductor near-coincident with a mineralised part of this sedimentary package. This shale unit is known to be variably mineralised, laterally extensive, and in this area has been mapped through geophysical logs as being very conductive where intersected by drilling. Whilst present at depth, there is no evidence, at present, to suggest it cannot be resolved by an airborne EM system such as that used here. There is ongoing debate as to whether these conclusions are valid, and further work is underway to determine whether the 1D, or the 3D results for that matter, produce artefacts and do not reflect reality, and whether the 2.5D outputs are, as Paterson *et al.* (2017) suggest, "superior".

It is well known that the geological suitability of inversion results requires their assessment against available geological information, rather than judgement made on the mathematical suitability of the inversion algorithm alone. Whilst the significance of the geological setting, its complexity, and the nature of the targets will have a bearing on how well different codes define a target, results from this investigation suggest that the 1D results can be interpreted with some confidence and can be used effectively in further exploration for sediment hosted base metal accumulations in the Batten Fault Zone in the southern McArthur Basin. The outcomes also indicate that when employing numerically complex inversion methods in the interpretation of AEM data sets, there may be significant value in asking a contractor/consultant for both 1D as well as higher order inversion results. In the resulting interpretations if conductors appear in one but not the other, then it is worth asking the question why?

ACKNOWLEDGMENTS

CSIRO Mineral Resources is acknowledged for supporting this research, and Marindi Metals Ltd. for providing access to their VTEM data set. The NTGS are also acknowledged for their support of the work through their CORE initiative.

REFERENCES

Auken, E., Christiansen, A.V., Kirkegaard, C., Fiandaca, G., Schamper, C., Behroozmand, A. A., Binley, A., Nielsen, E., Effersø, F, Christensen, NB, Sørensen, K., Foged, N. and Vignoli, G., 2015. An overview of a highly versatile forward and stable inverse algorithm for airborne, ground-based and borehole electromagnetic and electric data: Exploration Geophysics 46, 223–235. http://dx.doi.org/10.1071/EG13097

Ahmad, M., Dunster, J. N. and Munson, T. J., 2013. Chapter 15: McArthur Basin: in Ahmad M and Munson TJ (compilers). 'Geology and Mineral Resources of the Northern Territory'. Northern Territory Geological Survey, Special Publication 5.

Betts, P., Armit, R.J., and Ailleres, L., 2015. Potential-Field Interpretation Mapping of the Greater McArthur Basin. Pgn Geoscience Report 15/2014. *Geophysical and structural interpretation of the greater McArthur Basin.*

Christiansen, A.V. and Auken, E., 2012. A global measure for depth of investigation. GEOPHYSICS, 77, WB171–WB177.

Costelloe, M.T., Fitzpatrick, A., Roach, I.C. and Hutchinson D.K., 2013. EM Vision 3D inversion Data and Release Notes: Kintyre Area Subset of the Paterson Tempest AEM Survey W.A. Geoscience Australia.

Cox, L. H., Wilson, G. A. and Zhdanov, M. S., 2010. 3D inversion of airborne electromagnetic data using a moving footprint: Exploration Geophysics, 41, 250–259.

Ellis, R., 1998. Inversion of airborne electromagnetic data. Exploration Geophysics, 29, 121-127.

Flis, M. E., Newman, G. W., and Hohmann, G. W., 1989. Induced polarization effects in time-domain electromagnetic measurements: GEOPHYSICS, 5, 14-523.

Haber, E. Holtham, E., Granek, J., Marchant, D., Oldenburg, D., Schwarzbach, C. and Shekhtman, R., 2012. An adaptive mesh method for electromagnetic inverse problems. SEG Technical Program Expanded Abstracts 2012: pp. 1-6. doi: 10.1190/segam2012-0828.1

Kaminski, V. and Viezzoli, A., 2017. Modeling induced polarization effects in helicopter time-domain electromagnetic data: Field case studies. GEOPHYSICS, 82(2), B49-B61. https://doi.org/10.1190/geo2016-0103.1

Kang, S., Fournier, D., and Oldenburg, D.W., 2017. Inversion of airborne geophysics over the DO-27/DO-18 kimberlites —Part 3: Induced polarization. Interpretation. https://doi.org/ 10.1190/INT-2016-0141.1

Manca G. and Viezzoli A., 2018. A thorough synthetic study on IP effects in AEM data from different systems, AEGC 2018 Extended Abstracts, Sydney.

Paterson, R., Silic, J., and FitzGerald, D., 2016. Improved Structural Mapping and Conductive Targeting Delivered by a New 2.5D AEM Inversion Solver. ASEG Extended Abstracts 2016, 1-8. https://doi.org/10.1071/ASEG2016ab232

Paterson, R., Silic, J., FitzGerald, D. and Jakica, S., 2017. High accuracy 2.5D airborne electromagnetic inversion method for banded iron formation and other geological settings: AusIMM Iron Ore 2017, Perth, Australia, 24–26 July, 10pp.

Schwarzbach, C., Holtham, E. and Haber, E., 2013. 3D inversion of time domain electromagnetic data. ASEG Extended Abstracts 2013, 1-4. https://doi.org/10.1071/ASEG2013ab064

Shalley, M. J., and Harvey, T. V., 1992. Geophysical Response of the HYC Deposit, Exploration Geophysics, 23, 299-304.

Silic, J., Paterson, R., FitzGerald. D. and Archer, T., 2015. Comparing 1D and 2.5D AEM inversions in 3D geological mapping using a new inversion solver. 14th International, Congress of the Brazilian Geophysical Society, Extended Abstracts.

Silic, J., Paterson, R. and Fitzgerald, D., 2017. Inversion of AEM data at a survey scale utilising new inversion solver and forward model, PDAC 2017, Toronto, Canada.

Smith, R. S., 1989. Discussion on: "Induced polarization effects in time domain electromagnetic measurements": GEOPHYSICS, 54, 514–523, doi: 10 .1190/1.1442678.

Smith, R.S., 2016. Induced-polarization effects in airborne electromagnetic data: Estimating chargeability from shape reversals, SEG Technical Program Expanded Abstracts, pp. 2211-2217

Viezzoli, A., Kaminski, V. and Fiandaca, G., 2017. .Modeling induced polarization effects in helicopter time-domain electromagnetic data: Synthetic case studies. GEOPHYSICS, 82(2), E31-E50. https://doi.org/10.1190/geo2016-0096.1

Wilson, G.A., Raiche, A.P. and Sugeng, F., 2006. 2.5D inversion of airborne electromagnetic data. Exploration Geophysics, 37, 363-371.

Yang, D. and Oldenburg, D., 2012. Three-dimensional inversion of airborne time-domain electromagnetic data with applications to a porphyry deposit, GEOPHYSICS, 77 (2), B23-B34.

Yang, D., Oldenburg, D. and Haber, E., 2014, 3-D inversion of airborne electromagnetic data parallelized and accelerated by local mesh and adaptive soundings, Geophys. J. Int., 196 (3), 1492-1507

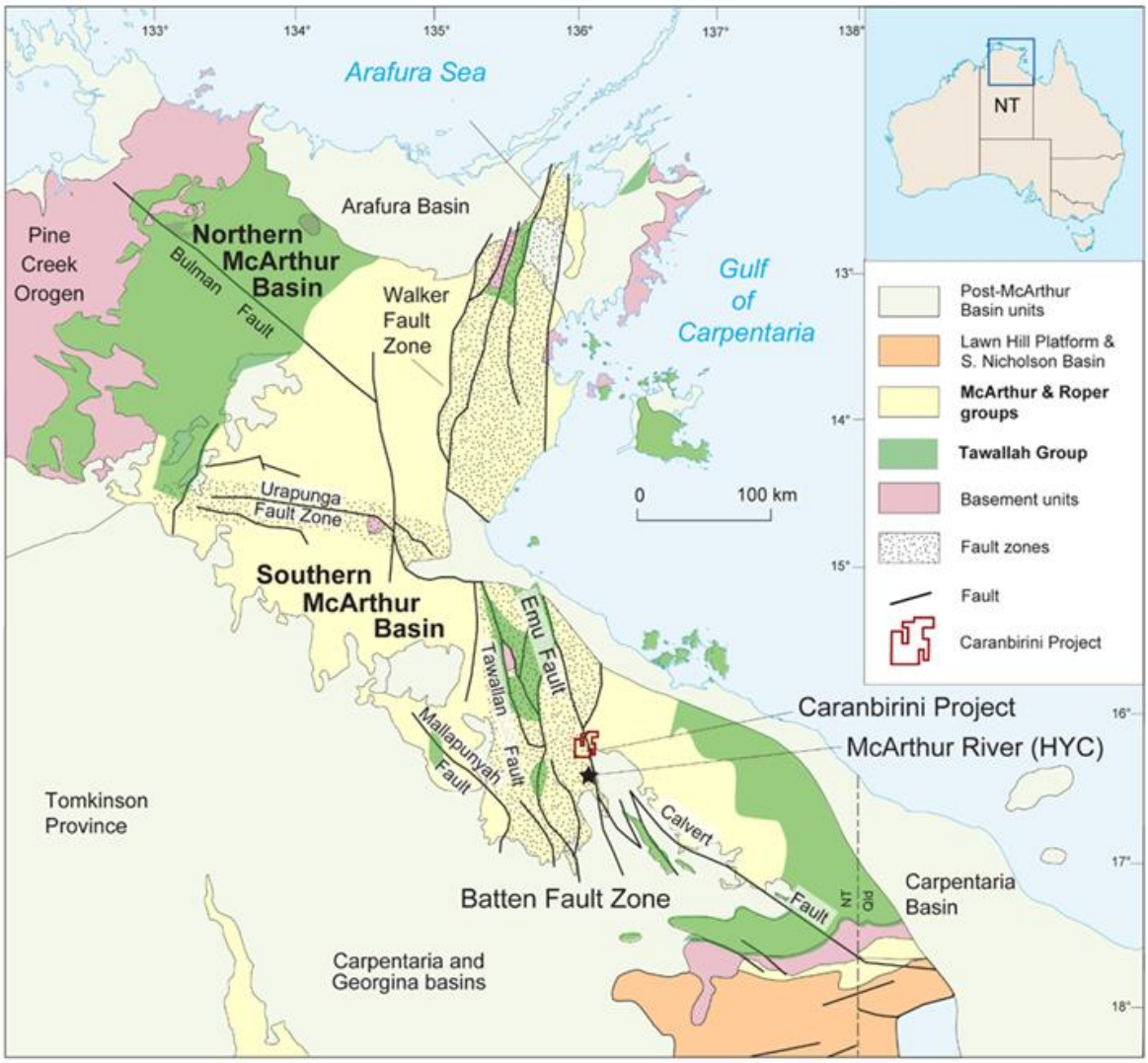

Figure 1: Simplified Geological map of the McArthur Basin. Basin sediments are divided into lower Tawallah Group, and undifferentiated McArthur and Roper Groups. The locations of the Caranbirini Project area straddling the Emu Fault is indicated. The location of the McArthur River (HYC) deposit is also shown. Map is modified after Ahmad et al. (2013)

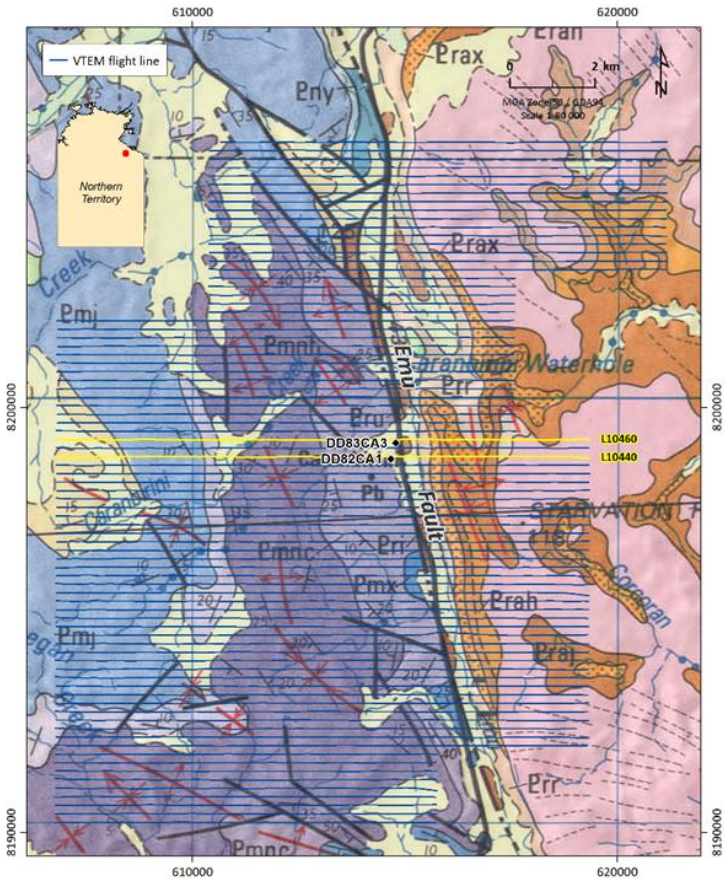

Figure 2: Flight line map for the Caranbarini AEM survey overlain on the regional geological map. The survey straddles the Emu Fault which marks the boundary between the Roper Group Sediments (east) and those of the McArthur Group (west).

Figure 3: System characteristics for AEM survey data acquired over Caranbirini Study site

VTEM MAX	
	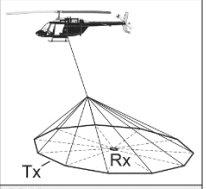
Survey Year flown	2010
Platform	Helicopter
System geometrical configuration	Concentric
	Suspended weight
Nominal heights Tx	Tx: 34 (m)
Rx	Rx: 34 (m)
Transmitter coil axis	Vertical
Tx loop area	962 (m^2)
Tx base frequency	25 (Hz)
Tx number of loop turns	4
Peak current	226 (A)
Peak dipole moment	870, 099 (NIA)
Nominal waveform shape	Half Sine-Trapezoid 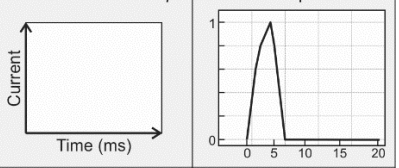
Duty cycle	28.67%
Tx height measured	Derived from helicopter
Tx orientation	GPS
Tx-Rx separations	Not measured (flexible frame)
Receiver orientation	Not measured
Receiver coils	X & Z
EM Sensor	dB/dt
# of receiver windows	36
EM channels mid times (ms)	0.083 to 10.667 (ms)

TMf005-17

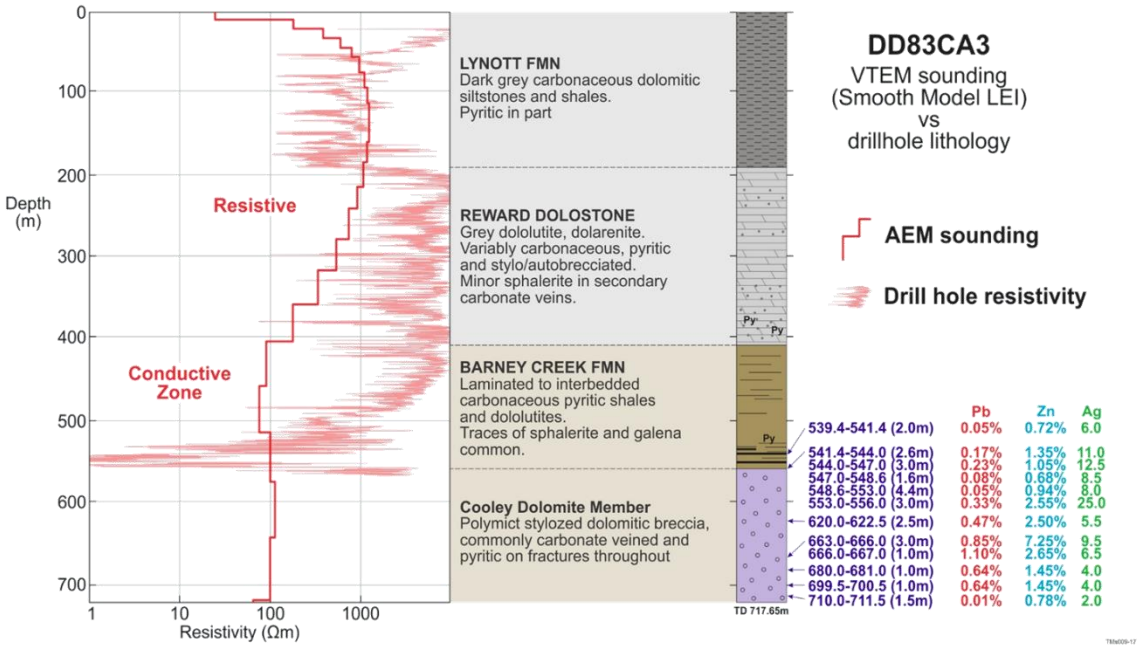

.

Figure 4: Lithology log (right) and 1D smooth model LEI inversion (left) for a VTEM fiducial closest to drill hole DD83CA3 on flight line 10460 (Figure 2). The hole drilled in 1983 by CRA Exploration Pty Ltd targeted a gravity high adjacent to the Emu Fault and logged McArthur Group stratigraphy. The cored stratigraphy consists of Lynott Formation, Reward Dolostone, Barney Creek Formation and the Cooley Dolomite Member The upper part of the sequence was modelled as a resistor, with the Barney Creek Formation becoming increasingly conductive with depth. The resistivity log for the hole indicated a very conductive unit in the lower Barney Creek Formation associated with the HYC Pyritic shale unit.

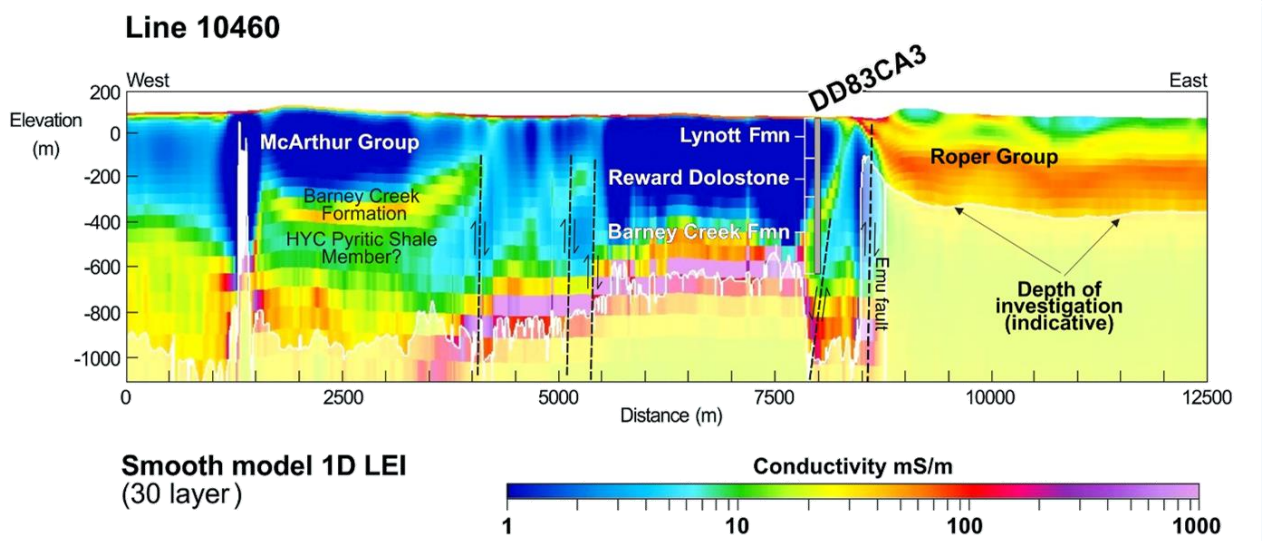

Figure 5: Conductivity depth section for a smooth model AarhusInv 1D LEI of Line 10460, showing a dipping conductor west of the Emu Fault which is intercepted by DD83CA3. Drillhole DD83CA3 was drilled in 1984 by CRA Exploration Pty Ltd and logged as McArthur Group stratigraphy. The cored stratigraphy consists of Lynott Formation, Reward Dolostone and Barney Creek Formation. The interpreted HYC Pyritic Shale member of the Barney Creek Formation was intercepted at a depth of ~540m below the ground surface.

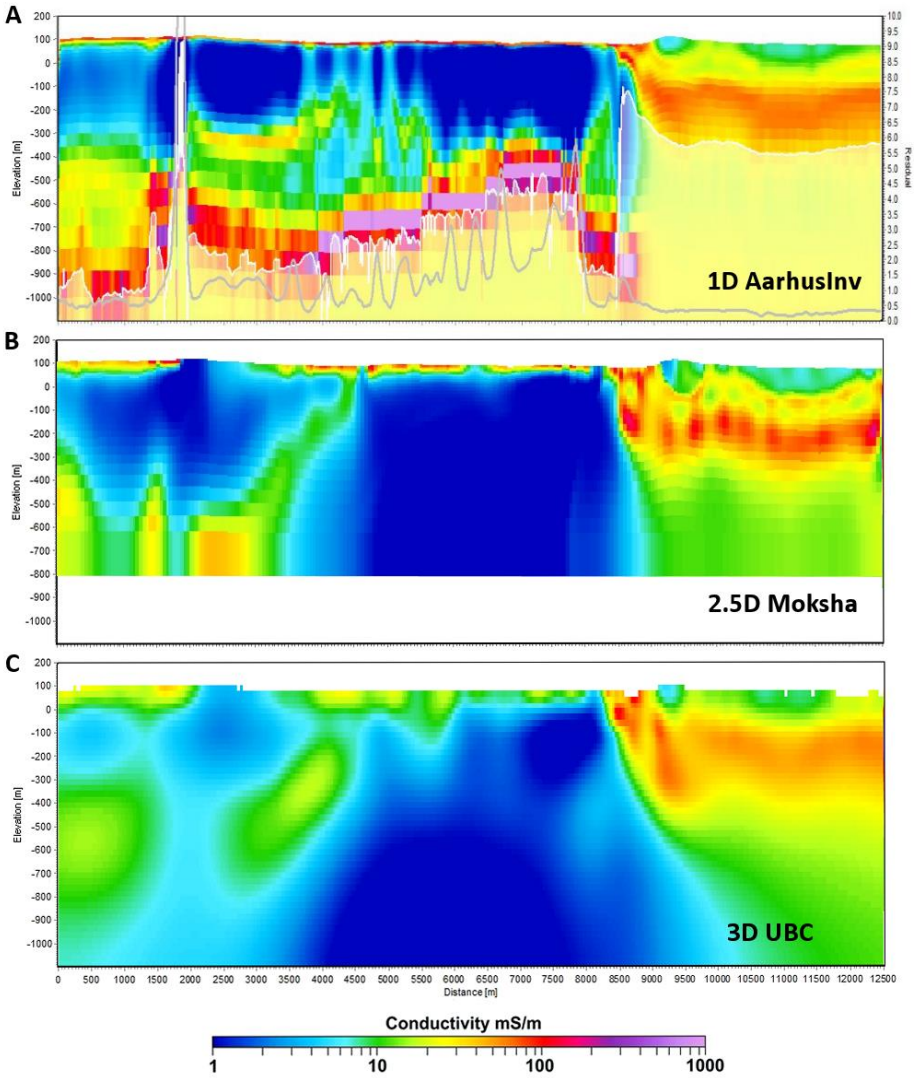

Figure 6: Conductivity-depth sections for line 10440, with results for three inversion approaches shown in the three panels. The top panel (A) is derived from the 1D smooth model inversion using AarhusInv; the middle (B) generated by Intrepid Geophysics using their 2.5D code; and the lower panel (C) using results from CGI's 3D inversion. The higher order inversion results produce smoother models with both suggesting the conductor at or just above the DOI (white line in Panel A) fitted in the 1D code may be an artefact. The dipping conductor representing Barney Creek Formation sediments intersected by drillhole DD83CA3 in Line 10460 to the north (see Figure 5), is also defined in the 3D results (albeit smoothed - between 8000 and 9000m). There is a hint of a conductor in the same position in the 2.5D section. Elsewhere (between 2500 and 6000m) the "folded" conductors, which have also been mapped in drillholes to the north as conductive HYC shale units, are not well resolved in either the 2.5 or 3D sections.

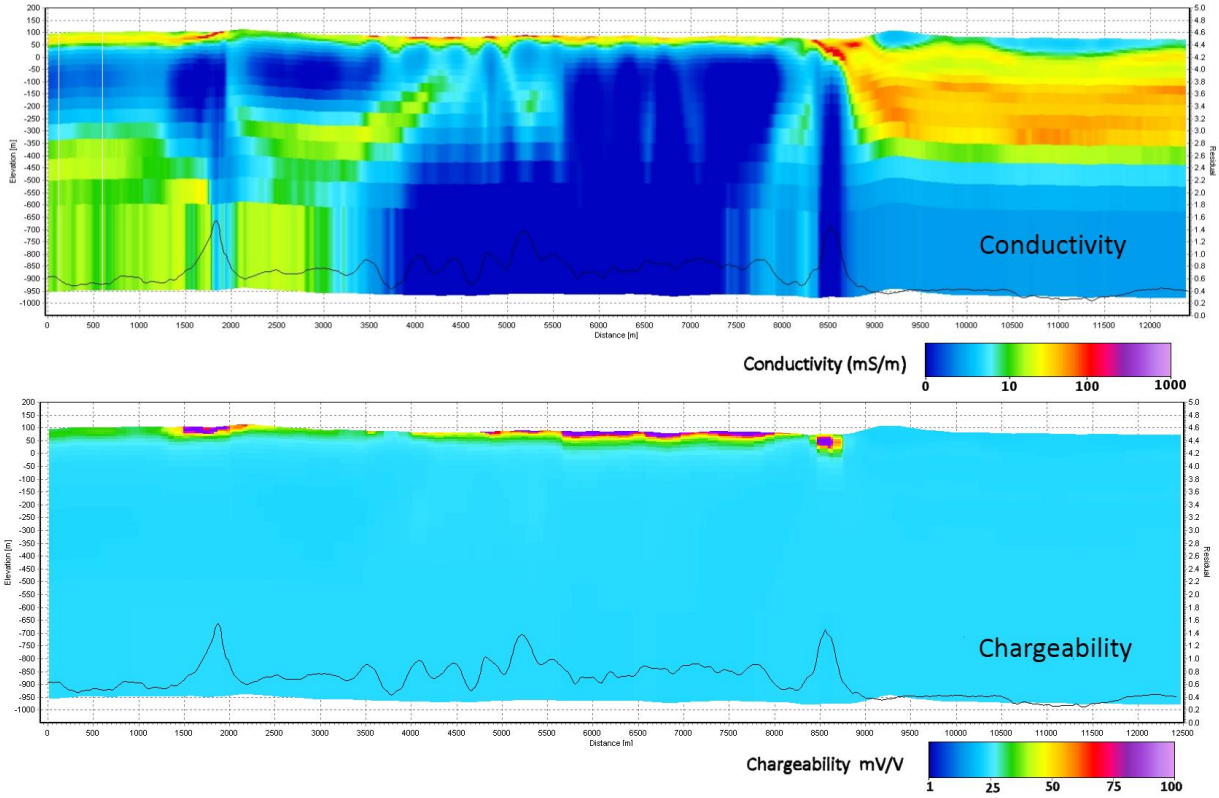

Figure 7: AarhusInv 1D inversion results for Line 10440 derived by solving for resistivity (conductivity), chargeability, frequency and a time constant together. Only the results for conductivity and chargeability with assocated misfit (black line in both plots), are shown. The inversion indicates that there are chargeable regolith (?) layers in the near surface, which are also conductive. The conductivity model is similar to that shown in Figure 6A, including what could be interpreted as folded conductors (between 4000 and 6000m). Only the deeper conductive layer in the middle of the section is missing. The data are well fitted throughout the section (particularly when compared with the data misfit in Figure 6A – grey line).

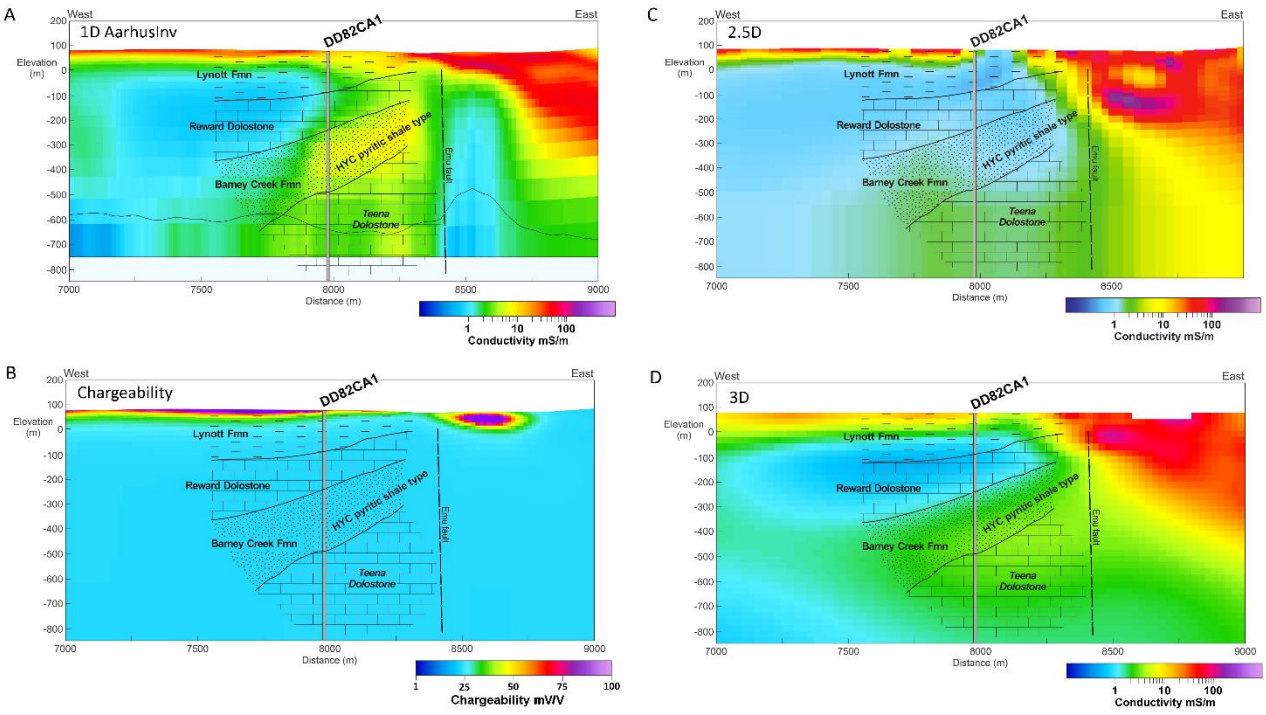

Figure 8: Enlarged section of Line 10440 (between 7000 and 9000m in Figure 7), for the area adjacent to the Emu Fault. The 1D inversion results (A) define a conductor associated with the HYC pyritic shale unit intersected in drillhole DD82CA1. A broad conductive zone is defined for that part of the stratigraphy and deeper in the 3D results (D), whereas the 2.5D inversion appears to define a more conductive zone at greater depth (C). A chargeable response is only defined in the near surface regolith (B).